analytical chemistry

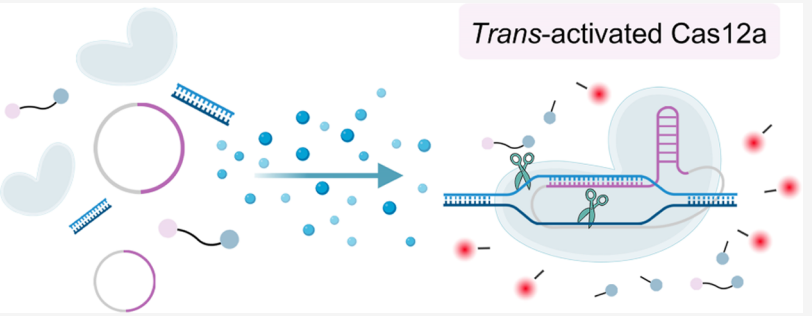
pubs.acs.org/ac Article

CrRNA Conformation-Engineered CRISPR-Cas12a System for Robust and Ultrasensitive Nucleic Acid Detection

Yueyuan Li, Qianfang Hu, Meiqi Bai, Min Qing,* and Lijuan Bai*

Cite This: *Anal. Chem.* 2025, 97, 3617−3624 Read Online

ACCESS | Metrics & More | Article Recommendations | Supporting Information



ABSTRACT: Despite the widespread application of the CRISPR-Cas12a system in vitro diagnostics due to its high programmability and distinctive *trans*-cleavage activity, the susceptibility of its crRNA component to degradation and sensitivity to storage and working conditions poses a significant challenge to improving the practical efficacy of these diagnostic systems. Here, we show that engineered crRNA with a covalently closed circular structure (C-crRNA) can replace traditional linear crRNA to form functional complexes with Cas12a protein, significantly enhancing the anti-interference ability of the CRISPR-Cas12a system while maintaining its sensitivity and specificity. Based on this finding, a circular crRNA-mediated CRISPR molecular diagnostic (CRCD) toolkit is developed and successfully integrated with a standard nucleic acid amplification technique to detect synthesized Human Papillomavirus type 16 (HPV-16) plasmids down to 10 aM sensitivity levels. Furthermore, the CRCD system is applied for ultrasensitive detection of 40 HPV-16 and 40 influenza A viruses in clinical samples, with results consistent with those from PANTHER detection and quantitative real-time polymerase chain reaction (qRT-PCR). In conclusion, this strategy introduces a novel paradigm for engineering crRNA to program Cas12a, which has the potential to revolutionize the use of crRNA in CRISPR-based molecular diagnostics.

Downloaded via SHANGHAI NORMAL UNIV on February 19, 2025 at 01:24:31 (UTC).
See https://pubs.acs.org/sharingguidelines for options on how to legitimately share published articles.

INTRODUCTION

The clustered regularly interspaced short palindromic repeats (CRISPR) system is an adaptive immune system for prokaryotes.[1−3] CRISPR technology has become a revolutionary toolkit in vitro diagnostics due to its high programmability and distinctive nuclease activity.[4−9] CRISPR RNA (crRNA) guides Cas protein to specifically target a complementary activator, after which Cas12a nicks the activator and indiscriminately digests nonspecific ssDNA.[10−13] Particularly, the highly efficient *trans*-cleavage activity of the Cas12a protein has been widely explored and successfully applied for the detection of various pathogens.[10,14−17] Moreover, the high programmability of Cas12a has led to the development of innovative biosensors, expanding the application scope of CRISPR technology beyond nucleic acid targets.[18−20]

The CRISPR-Cas12a system comprises Cas protein and crRNA, with the integrity of these components being essential for the functional lifespan and the effectiveness of CRISPR-based assays. However, crRNA's inherent properties, including a short half-life, make it a relatively fragile component of the CRISPR system. It is highly prone to degradation by ribonucleases, which are ubiquitous in various environments and sample matrices.[21,22] Additionally, in practical clinical sample testing, the CRISPR system usually involves complex operational procedures and the addition of various reagents and necessitates specialized laboratories. These limitations may significantly restrict the application scenarios of CRISPR-based molecular diagnostic technologies and their compatibility with various portable detection technologies.[23] Consequently, building a robust CRISPR system often requires a rational design and meticulous optimization.

Received: November 12, 2024
Revised: January 29, 2025
Accepted: January 30, 2025
Published: February 6, 2025



ACS Publications © 2025 American Chemical Society

https://doi.org/10.1021/acs.analchem.4c06107
Anal. Chem. 2025, 97, 3617−3624

It is precisely because the crRNA is a less stable component in the CRISPR-Cas12a complex that it is usually engineered to enhance the stability of the CRISPR system. Modifying the backbone of crRNA is a conventional strategy to improve RNA stability, including 2′-O-methyl-3′-phosphonoacetate, locked nucleic acid, and replacement of ribonucleotides with deoxyribonucleotides.[24−28] Nonetheless, the existing modification strategies, which often require intricate and expensive chemical syntheses as well as specialized procedures, are challenging to implement in many standard laboratories. Alternatively, exploring the topological structure of RNA to enhance stability represents another strategy. Nelson et al. engineered guide RNA with pseudoknots to protect from degradation.[29] Zhang et al. and Liu et al. in vivo synthesized guide RNA with covalently closed circular structure to enhance the stability of gene editing.[22,30] However, little is known about the *trans*-cleavage efficiency of circular crRNA-guided Cas12a and whether circular crRNA can replace linear crRNA to form complexes with Cas12a to enhance the anti-interference ability of CRISPR-Cas12a systems. Circular RNA (circRNA), a newly identified category of noncoding RNAs in eukaryotic organisms, is arose from the back-splicing of precursor mRNA.[31,32] Predominantly composed of exons, circRNA is characterized by the covalently closed circular structure.[33] The absence of 5′ end-caps nor 3′ end poly(A) tail in circRNA enables it to evade deadenylation and decapping, and the distinctive structure of circRNA reduces the probability of circRNA being recognized and degraded by the cellular RNA decay mechanisms.[34] Furthermore, the lack of free ends in circRNA confers an increased resistance to exonucleases, which contributes to its extended half-life relative to linear RNA.[35,36]

Inspired by the inherent stability of circRNA, our study utilized a simple biotechnological technique to circularize linear crRNA (L-crRNA), confirming that the optimized circular crRNA (C-crRNA) is more resistant to ribonuclease digestion while maintaining comparable sensitivity and specificity. By integrating C-crRNA with the CRISPR-Cas12a system, we developed a more robust CRISPR-Cas12a detection system, termed the circular crRNA-mediated CRISPR molecular diagnostic (CRCD) toolkit. We further validated that our CRCD platform is capable of detecting synthesized Human Papillomavirus type 16 (HPV-16) plasmids with a concentration as low as 10 aM within 60 min. Ultimately, we implemented the CRCD system for the ultrasensitive detection of HPV-16 and influenza A virus in clinical samples and extended the technology to lateral flow analysis to meet point-of-care criteria. The clinical sample testing presented above validates the practical applicability of the CRCD system.

EXPERIMENTAL SECTION

Preparation of C-crRNA. Brief, the circularization of crRNA was performed using 1× T4 RNA Ligase Reaction Buffer (50 mM Tris−HCl, 10 mM $MgCl_2$, 1 mM DTT, and 40 μM ATP), 5′-phosphorylated linear crRNA (50 pmol), 50 U (units) of T4 RNA ligase 1, 20 U of RNase inhibitor, 10% PEG8000 and RNase-free water to a total volume of 20 μL. After incubation at 25 °C for 1 h, the obtained C-crRNA molecules were analyzed by 12% polyacrylamide gel electrophoresis (PAGE) to identify the target RNA band. Then, the gel block was transferred to the blue light cutter (LABGIC, China). The target bands were then excised with a clean blade, transferred to centrifuge tubes, and crushed with a disposable pestle. Nucleic acid extraction and purification were carried out using the HiPure Poly gel RNA Kit according to the manufacturer's protocol. Finally, the purified RNA was subsequently quantified using the NanoPhotometer N60 Touch (Implen GmbH, Germany).

***trans*-Cleavage of CRISPR-Cas12a Assays.** In a 20 μL reaction system, Cas12a (10 nM) and crRNA (10 nM) were preincubated with target DNA in the 1× NEBufferTM r2.1 buffer at 37 °C for 20 min to form ternary complexes, followed by the addition of ssDNA FQ reporter with a final concentration of 250 nM. Each Reaction was conducted in three replicates to ensure reliability of the results. The real-time fluorescence was detected by a CFX Connect Real-Time PCR Detection System (Bio-Rad) at 37 °C for 1.5 h, with signals being recorded every 30 s.

***cis*-Cleavage of CRISPR-Cas12a Assays.** For the *cis*-cleavage assay, a 10 μL reaction mixture was prepared with 1 μL of 10× NEBuffer r2.1 buffer, 1 μL of Cas12a (1 μM), 1 μL of crRNA (1 μM), 1 μL of PCR amplicons, and 6 μL of RNase-free water. The Cas12a and crRNA were preincubated at room temperature for 30 min before being mixed with PCR products. The mixture was then incubated at 37 °C for 60 min. The reaction was stopped by heating the mixture to 65 °C for 10 min, and the products were visualized on PAGE gels.

RNase R Digestion Assay. For the RNase R digestion assay, a 20 μL reaction mixture containing 2 μL of 10× RNase R buffer, 1 μL of RNase R (2 U/μL), 10 μL of crRNA (1 μM), and 7 μL of RNase-free water was incubated at 37 °C for 0, 0.5, 1, 2, 4, 8, 12, and 24 h. The reaction was stopped by heating at 80 °C for 10 min, and the products were analyzed by PAGE assays and *trans*-cleavage.

Human Clinical Sample Detection. The study was approved by the Ethics Committee of Chongqing Medical University (reference number: 2024128). A total of 40 human cervical cell samples and 40 IVA samples were collected. A crude DNA preparation was made using a nucleic acid extraction or purification reagent. The kit employs the Chelex 100 high-temperature method to rapidly lyse cells and release genomic DNA. The Influenza A and B virus nucleic acid detection Kit was used to extract IVA RNA from clinical samples in a biosafety level II laboratory. The human cervical cell samples were assayed in the clinical laboratory using the PANTHER detection system (HOLOGIC Corporation, America), while IVA samples were tested using the standard quantitative real-time polymerase chain reaction (qRT-PCR) method. Prior to the CRCD assay, 2 μL of the sample's nucleic acid extract was amplified by PCR or RT-PCR, and then 2 μL of the amplicon was immediately added to the CRCD system for fluorescence detection. For the lateral flow assay, the *trans*-cleavage step was performed as described above, with the exception of using a FAM-biotin reporter instead of the original FQ reporter. After the reaction was completed, 30 μL of ultrapure water was added to achieve a final volume of 50 μL. A CRISPR lateral flow strip was then dipped in each reaction mixture and allowed for rapid visualization.

RESULTS AND DISCUSSION

Engineered C-crRNA-Mediated Activation of Cas12a. Previous study has employed the Tornado expression system to generate circular guide RNA (cgRNA) intracellularly.[22] However, the Tornado expression system can only be applied in vivo, which undoubtedly limits the in vitro applications of

https://doi.org/10.1021/acs.analchem.4c06107
Anal. Chem. 2025, 97, 3617−3624

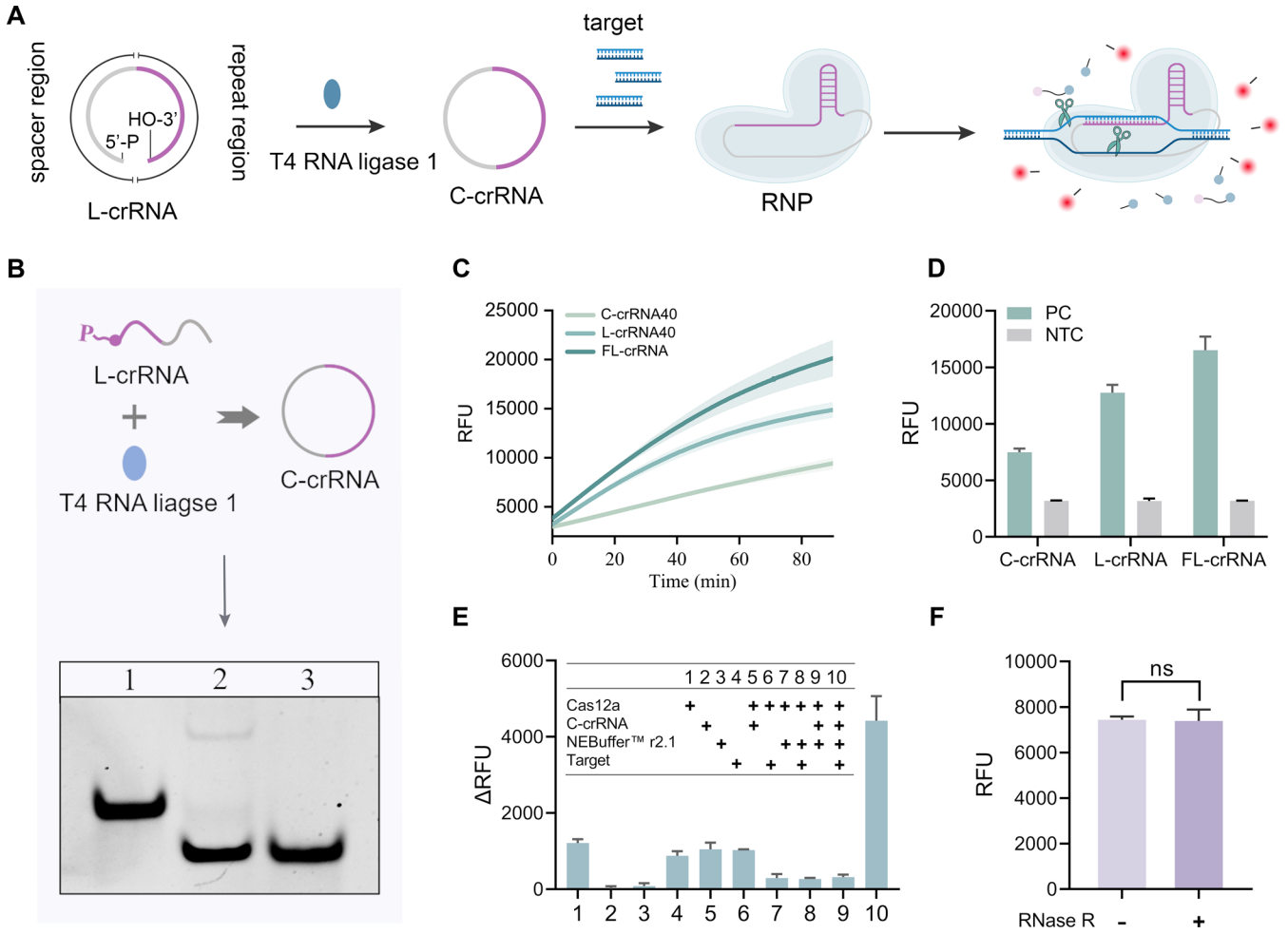


Figure 1. (A) Schematic diagram of the CRCD platform for nucleic acid detection. (B) PAGE analysis of C-crRNA. Lane 1: L-crRNA40, lane 2: enzymatic ligation of L-crRNA40 followed by RNase digestion, lane 3: gel-purified C-crRNA40. The top panel is a schematic diagram of C-crRNA synthesis. (C) Real-time fluorescence curves for detecting synthesized HPV-16 plasmids using three different crRNAs. (D) Histogram depicts the fluorescence intensity at 60 min. (E) Components deletion experiment. The histogram shows the difference in fluorescence intensity between experimental groups (1−10) at 60 min. The ΔRFU was determined by subtracting the background fluorescence of the probe-only group from the total fluorescence intensity of the experimental group. (F) Histogram shows the comparison of fluorescence intensity before and after RNase R digestion. PC, positive sample, NTC, negative sample. ns, not significant. Data are represented as the mean ± SD (n = 3 replicates).

the CRISPR system. Therefore, we aimed to engineer crRNA to achieve a stable RNA conformation, thereby creating an enhanced CRISPR system (Figure 1A). To test our hypothesis, we initially carried out the circularization of the L-crRNA using T4 RNA ligase 1, which catalyzes the generation of an intramolecular linkage between the 5′-phosphate and the 3′-hydroxyl of an oligoribonucleotide. Table S1 shows the widely used full-length crRNA (FL-crRNA), which consists of a 21 nucleotide (nt) direct repeat region and a 20 nt spacer region for target recognition. Since RNA with a 3′ end cytosine is not a suitable substrate for T4 RNA ligase 1, we synthesized a 40 nt crRNA (comprising a 21 nt repeat sequence and a 19 nt spacer region) for preliminary validation. The successful preparation of C-crRNA was first evaluated by 12% PAGE. As shown in Figure 1B, lane 1 represents the characteristic band of linear crRNA40 (L-crRNA40). After an enzymatic ligation and Ribonuclease R (RNase R) treatment, a band migrating faster than L-crRNA40 is observed (lane 2), which is assigned to the characteristic band of circular crRNA40 (C-crRNA40). Since RNase R is a 3′-to-5′ exoribonuclease that digests linear RNA and hardly digests circular RNA, the presence of the characteristic band of C-crRNA40 in lane 2 further confirms the successful preparation of C-crRNA40. However, a small quantity of larger circular byproducts is still observed, appearing as a band positioned above the C-crRNA40 band. To eliminate the potential impact of these byproducts, we purified the C-crRNA40 from PAGE gels to obtain the gel-purified C-crRNA40 (lane 3).

To validate whether C-crRNA could assemble with Cas12a to form a complex that recognizes the target, thereby activating the *trans*-cleavage activity of CRISPR-Cas12a, we conducted a fluorescence assay using a plasmid containing the HPV-16 gene as the target. For signal readout, we used a FRET-based reporter consisting of a 6-carboxyfluorescein (HEX) and a black hole quencher 1 (BHQ1) connected by a 12 nt sequence (TTATTTATTTAA), termed the FQ reporter, which produces enhanced fluorescence upon *trans*-cleavage. As shown in Figure 1C,D, C-crRNA40 can activate the CRISPR system, albeit with slightly lower intensity compared to L-crRNA40. Comparing the fluorescence intensities of the FL-crRNA and the L-crRNA40 indicates that a reduction in the length of the spacer region leads to a decrease in fluorescence

https://doi.org/10.1021/acs.analchem.4c06107
Anal. Chem. 2025, 97, 3617−3624

intensity, which is consistent with previous research.[10] To preclude the potential influence of 5′-phosphate modification of crRNA on the CRISPR-Cas12a system, we also compared the fluorescence signals of 5′-phosphorylated and non-phosphorylated crRNAs. For identical crRNA sequences, the CRISPR-Cas12a system showed no significant distinction between 5′-phosphorylated and nonphosphorylated crRNAs (Figure S1). Subsequently, we conducted *cis*-cleavage assays (Figure S2). The PAGE analysis results confirm concordance with those of the *trans*-cleavage assay. Moreover, we performed a component deletion experiment. The results demonstrate C-crRNA as a key component mediating Cas12a activation with high specificity (Figure 1E). In addition, considering the possibility of residual L-crRNA in the gel-purified C-crRNA, which could also contribute to increased fluorescence intensity, we treated the C-crRNA with RNase R. The results reveal that the generation of a fluorescent signal is indeed based on the presence of C-crRNA (Figure 1F). Overall, the above results suggest that C-crRNA can mediate the activation of Cas12a.

Enhanced Ribonuclease Resistance of C-crRNA. Cas12a is a crRNA-guided nuclease, and its *trans*-cleavage activity is activated only when the crRNA guides it to bind to the activator. The stability of gRNA during storage and application is a crucial factor in determining the effectiveness of the CRISPR-based assays. To assess the ribonuclease resistance of L-crRNA and C-crRNA, we first exposed both types of crRNA to RNase R for varying durations and then analyzed the samples via PAGE. Significantly, the characteristic band of L-crRNA is barely detectable after 30 min of digestion, indicating rapid degradation of the linear form (Figure 2A). In contrast, C-crRNA remains visible even after a 12 h of incubation (Figure 2B). We further conducted fluorescence assays to measure degradation efficiency at different time intervals. Concurrently, the *trans*-cleavage assays for Cas12a-L-crRNA complex reveal a significant decline in *trans*-cleavage efficiency to 30.1% ± 0.5% after 30 min of exposure to RNase R (Figure 2C). In contrast, the Cas12a-C-crRNA complex sustains an average *trans*-cleavage efficiency of 75.2% ± 0.3%. Even after an extended 8 h incubation, the Cas12a-C-crRNA complex preserves nearly half of its initial cleavage capacity, while the Cas12a-L-crRNA complex almost completely loses its cleavage activity (Figure 2D). These results demonstrate the superior stability of C-crRNA, indicating its potential to outperform L-crRNA in applications of the CRISPR technology. Furthermore, we employed RNase R to simulate ribonuclease contamination during the detection process. As shown in Figure S3, the fluorescence intensity of the conventional CRISPR system markedly decreased with the increase of RNase R, which is attributed to the degradation of crRNA by RNase R, leading to a decrease in the formation of Cas-crRNA functional complexes in the system. The enhanced resilience of C-crRNA against ribonuclease degradation may lead to more reliable and reproducible outcomes in CRISPR-based assays.

C-crRNAs with Different Lengths Affecting Cas12a *trans*-Cleavage Activity. The *trans*-cleavage experiments indicate that the activity of the Cas12a-C-crRNA complex is slightly lower than that of the Cas12a-FL-crRNA complex. Initially, we hypothesized that the diminished *trans*-cleavage activity might be ascribed to the additional preprocessing of circular crRNA by Cas12a. It has been reported that Cas12a is able to process precursor crRNAs (pre-crRNAs) through its own nuclease activity to generate mature crRNAs.[37−39] These

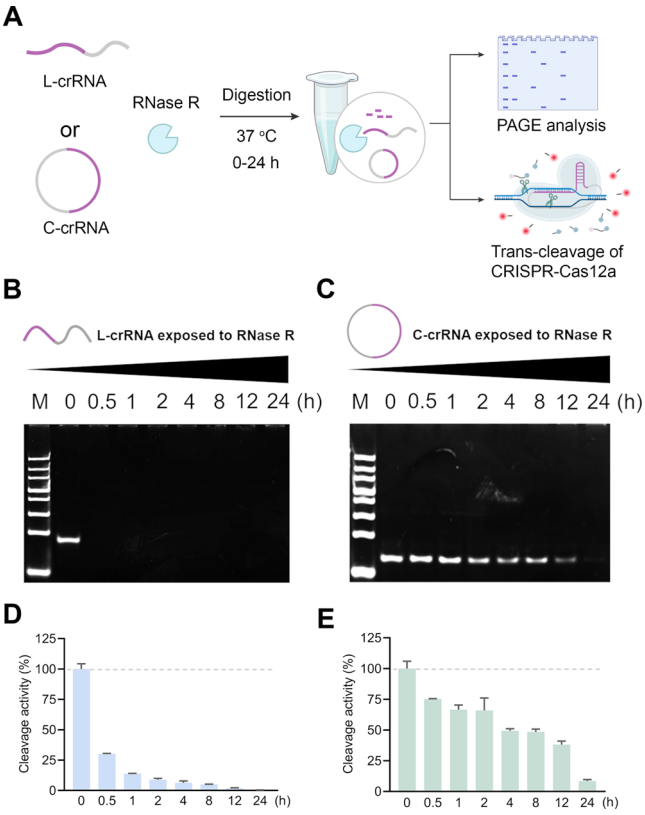


Figure 2. Ribonuclease resistance assay. (A) Schematic workflow of L-crRNA40 and C-crRNA40 targeting the HPV-16 gene treated with RNase R. 12% PAGE analysis of equal molar (B) L-crRNA40 and (C) C-crRNA40 after incubation with RNase R for different times. Cleavage activity of the CRISPR system based on incubation of (D) L-crRNA40 and (E) C-crRNA40 with RNase R for different times. Data are represented as the mean ± SD (n = 3 replicates).

mature crRNAs can subsequently bind to Cas12a proteins to form an active ribonucleoprotein complex. Figure S4 indicates that Cas12a does not preprocess circular crRNAs. We therefore suggest that this reduced signal may be attributed to the conformational restriction imposed by the circular structure of the C-crRNA, which could mildly impede its affinity for Cas12a or decelerate the target recognition process. Based on this hypothesis, we speculate that increasing the length of C-crRNA might enhance its *trans*-cleavage activity. Therefore, we engineered C-crRNA by extending the spacer region with different lengths of uridinylates. Concurrently, to explore the effect of C-crRNA length on Cas12a activation, we reasonably designed truncated crRNA based on the principle that the 3′ end should not contain cytosine (Table S1). The top panel of Figure 3A illustrates the schematic diagram of these engineered C-crRNAs with lengths ranging from 37 to 51 nt. As can be seen from Figures 3A and S5, the fluorescence signal increases with the length of C-crRNA and approaches that of FL-crRNA when the length reaches 51 nt.

Furthermore, to elucidate the enzymatic activity of Cas12a triggered by FL-crRNA and C-crRNA51, we conducted a Michaelis−Menten kinetic study using varying concentrations of FQ reporters (Figures 3B,C, and S6). The results indicate that the catalytic efficiency (k_{cat}/K_m) for the Cas12a-C-crRNA51 complex is comparable to that of the Cas12a-FL-crRNA complex. The detailed kinetic parameters are shown in Table S5. Therefore, to navigate the trade-off between stability

https://doi.org/10.1021/acs.analchem.4c06107
Anal. Chem. 2025, 97, 3617−3624

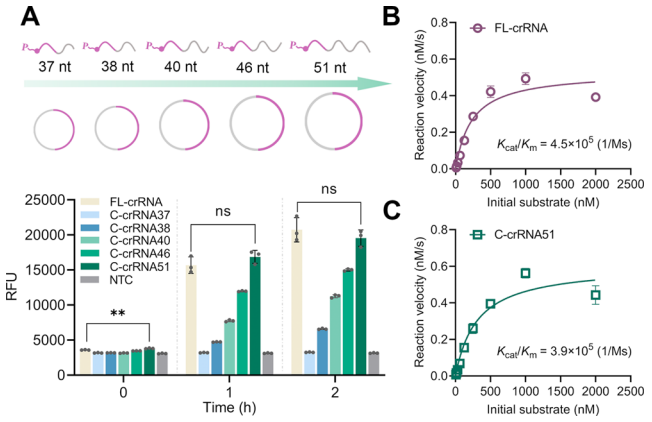


Figure 3. (A) Top panel shows the schematic diagram of the engineered C-crRNAs with lengths ranging from 37 to 51 nt. The histogram compares the *trans*-cleavage activity of C-crRNAs of varying lengths. The Michaelis−Menten plots for *trans*-cleavage activity induced by (B) Cas12a-FL-crRNA complex and (C) Cas12a-C-crRNA51 complex. NTC, negative sample. ns, not significant, $^{**}p < 0.01$. Data are represented as the mean ± SD (n = 3 replicates).

and sensitivity in the CRISPR system, we selected the 51 nt C-crRNA to replace the traditional FL-crRNA as the core component to construct our enhanced CRISPR detection method, a circular crRNA-mediated CRISPR molecular diagnostic (CRCD) system.

Analytical Performance of the CRCD System. Prior to the formal testing, we optimized the key parameters of the CRCD method, including the preincubation time of the ternary complex and the ratio of Cas12a-C-crRNA51 (Figure S7). As a proof of concept, the plasmid containing the HPV-16 gene was serially diluted to obtain activators at varying concentrations, thereby verifying the detection performance of our method. The results show that the Limit of Detection (LoD) for both the conventional CRISPR-Cas12a system and the CRCD system is 5 pM, suggesting that C-crRNA51 has the potential to replace FL-crRNA (Figure 4A,B). Besides, we also compared the LoD of the two systems in the presence of RNase R (Figure S8). The results show that the sensitivity of the CRCD system (5 pM) is enhanced about 10-fold compared to the conventional CRISPR system (50 pM). To improve the sensitivity, we combined a nucleic acid preamplification. As illustrated in Figures S9 and S10, with the combination of canonical PCR amplification, the optimized CRCD-PCR assay allows for a LoD as low as 10 aM. This result demonstrates that the sensitivity of the CRCD-PCR system has been improved by nearly 6 orders of magnitude over the nonamplified system.

In addition to high sensitivity, good specificity also determines whether C-crRNA can serve as a core component of the proposed enhanced CRISPR system. Previous studies have shown that CRISPR-Cas12a is sensitive to target sequences and has promising specificity. Therefore, for the first time, we assessed the specificity of the C-crRNA-based CRISPR system, using a series of activators containing single base mutations (Table S6). We designed a hairpin DNA that is fully complementary to the crRNA spacer region as the wild-type (WT) activator, characterized by a double-stranded stem stabilized by a loop structure. Additionally, a single base mutation was introduced at different positions (1, 3, 6, 9, 12, 15, 18) within the target sequence that is complementary to the crRNA spacer region (Figure 4C). The results indicate that

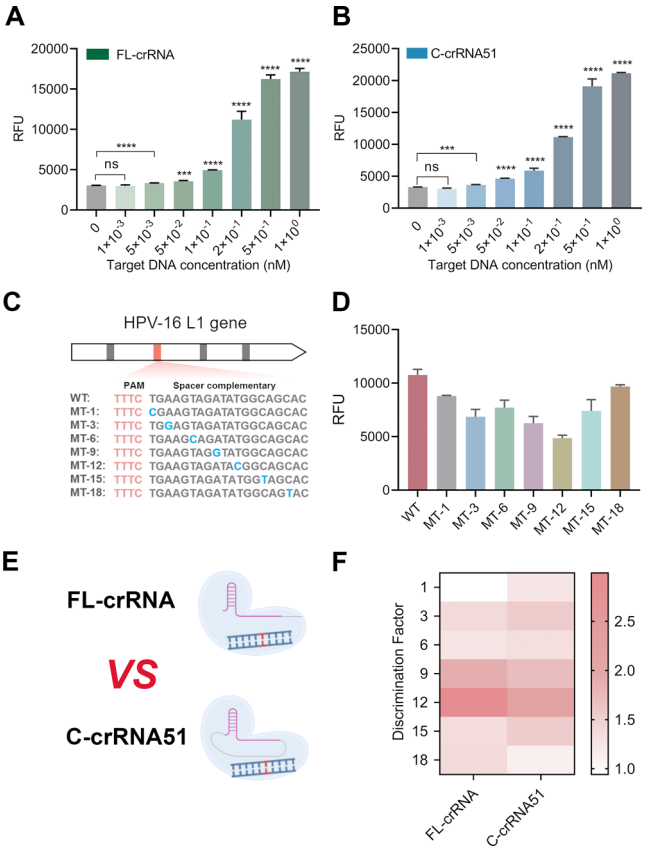


Figure 4. Sensitivity analysis of (A) the conventional CRISPR-Cas12a system and (B) the CRCD system. (C) The complementary sequence (WT) and mismatch sequences (MT-1−MT-18). (D) End point fluorescence intensity for detection of complementary sequence (WT) and mismatch sequences (MT) using the CRCD system at 60 min. (E) Schematic diagram comparing the specificity of the two systems. (F) Heat map of the specificity tests of the conventional CRISPR-Cas12a system and CRCD system. Discrimination factor formula: DF = (F_{WT} − background)/(F_{MT} − background). NTC, negative sample. $^{***}p < 0.001$, $^{****}p < 0.0001$, ns, not significant. Data are represented as the mean ± SD (n = 3 replicates).

the CRCD system has a good single nucleotide sensitivity (Figures S11 and 4D). Moreover, the specificity of the system was evaluated using the DF value (discrimination factor, indicative of the capacity to differentiate between target and interfering strands with only a single base difference). As shown in Figure 4E,F, the specificity of the two systems did not exhibit significant differences, and the CRCD system demonstrated better specificity at positions 1, 3, 6, and 15. In summary, the CRCD system has comparable sensitivity and specificity to the conventional CRISPR-Cas12a system, especially with superior stability, features that give it significant application potential in molecular diagnostics.

Clinical HPV-16 Sample Detection by the CRCD System. To verify the qualification of the CRCD system for molecular diagnosis, we directly detected the viral genome to assess the practicality of this method. Notably, HPV-16 is one of the most predominant subtypes causing cervical cancer, and it is critical for early diagnosis and treatment of cervical cancer.[40−43] In this study, clinical research was conducted using cervical swab samples. The PANTHER detection system, certified by CFDA, was utilized to genotype 40 collected samples, identifying 24 HPV-16 positive and 16 negative

https://doi.org/10.1021/acs.analchem.4c06107
Anal. Chem. 2025, 97, 3617−3624

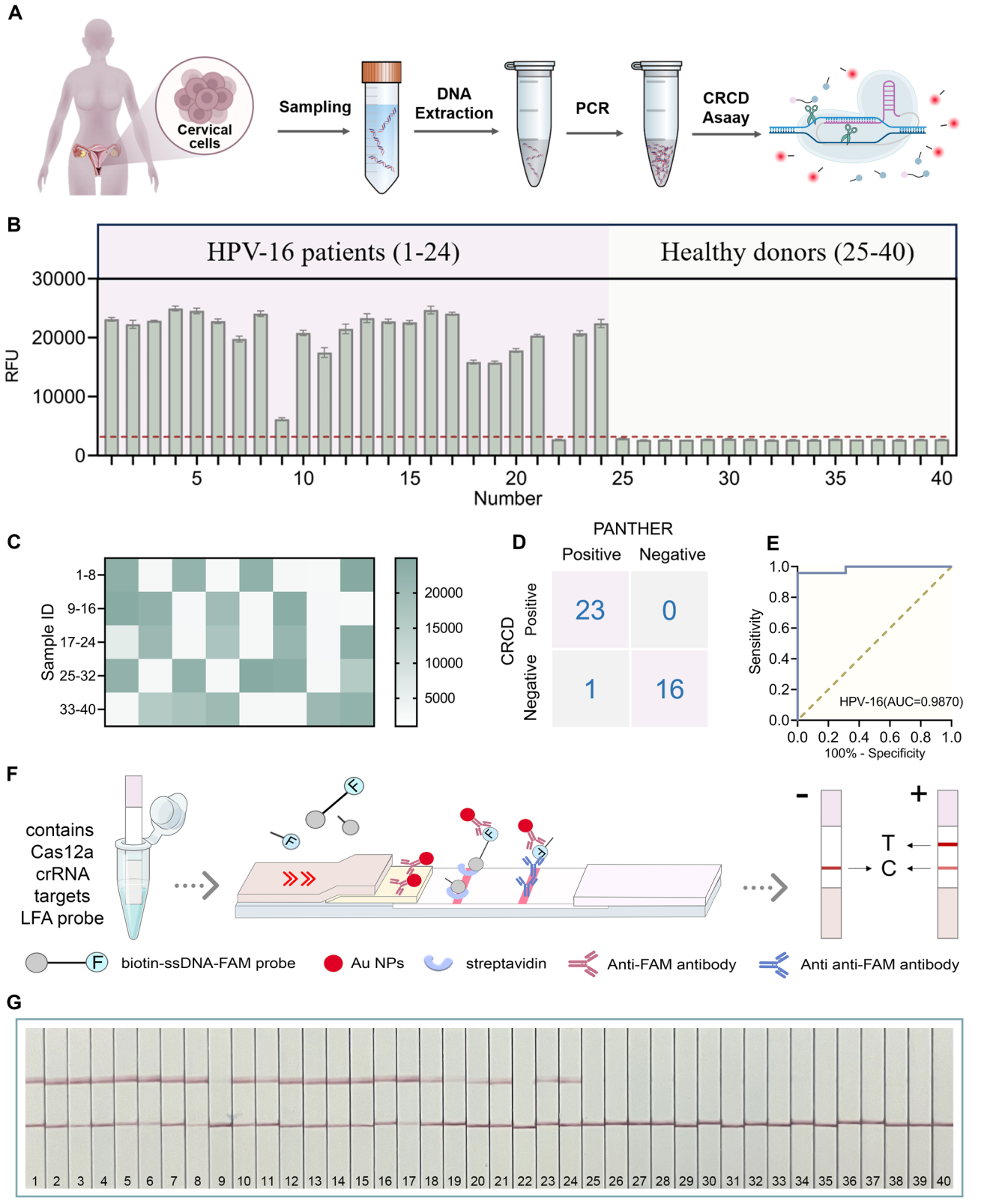


Figure 5. (A) Schematic illustration of the analysis of HPV-16 infected clinical samples by CRCD. (B) HPV-16 detection in 40 cervical swab samples. The red dotted line represented the threshold for a positive sample, which was calculated from the average fluorescence plus 3 SDs of NTC. (C) Heat map shows the results of the CRCD system on the detection of 40 cervical swab samples. (D) Evaluation of CRCD sensitivity and specificity compared with standard PANTHER system. (E) ROC curve analysis of the detection accuracy in clinical applications. (F) Principle of CRCD-LFA. (G) Test results of lateral flow assay of 40 cervical swab samples. Data are represented as the mean ± SD (n = 3 replicates).

samples (Table S7). The workflow of our method for clinical sample detection is depicted in Figure 5A. The identification of positive and negative samples by the CRCD system is based on a threshold value, and the results are shown in Figure 5B,C. As

https://doi.org/10.1021/acs.analchem.4c06107
Anal. Chem. 2025, 97, 3617−3624

can be seen, twenty-three out of 24 positive samples were successfully identified by the CRCD system within a 20 min test, with only one case remaining undetected. The sensitivity and specificity obtained by this method were 95.8 and 100%, respectively (Figure 5D). The receiver operating characteristic (ROC) curve demonstrated an AUC value of 0.9870, which confirms the excellent diagnostic performance of the CRCD system (Figure 5E). Additionally, the selectivity of the detection method is also important. Therefore, we collected several other common high-risk HPV subtypes and used PCR primers and crRNA targeting the HPV-16 gene for detection. As shown in Figure S12, no other subtypes were detected with only HPV-16 being identified. In summary, the CRCD system is applicable for HPV detection in clinical samples, exhibiting good sensitivity and accuracy.

In addition, the point-of-care capability of the developed CRCD system was demonstrated by integrating the lateral flow assay (LFA) (Figure 5F). The lateral flow readings demonstrated that the CRCD-LFA system effectively distinguished between positive and negative samples, aligning with the PANTHER results (Figure 5G). The results highlight the suitability and potential of the CRCD system for point-of-care applications.

Clinical IVA Sample Detection by the CRCD System. To further expand the applications of the CRCD system, we believe that the CRCD system should also be applicable to RNA detection. IVA is a highly contagious disease, emphasizing the need for robust nucleic acid detection strategies.[44,45] We collected 40 throat swab samples and compared our CRCD system with qRT-PCR, which is the gold standard for diagnosing IVA (Table S8).

The clinical samples from 30 patients infected with IVA were identified using the qRT-PCR method (Figure S13). For our method, we designed a 51 nt crRNA (crFlu51) based on the sequence of the IVA gene and circularized it for use. Subsequently, we tested its *trans*-cleavage activity compared to that of traditional crRNA to validate the versatility of the CRCD toolkit. Figure S14 shows that Cas-C-crFlu51 still possesses excellent cleavage activity, although the activity is slightly lower than that of conventional crRNA, which may be due to the different sequence compositions with different binding affinities for the target sequences and Cas protein. After RT-PCR primer optimization, we conducted actual sample assays using CRCD-RT-PCR (Figures S15 and S16A). As shown in Figure S16B,D, our method was able to effectively detect 30 positive samples within 20 min, yielding a sensitivity of 100% and a specificity of 100%. Moreover, the results from the CRCD method are almost consistent with those from qRT-PCR. The ROC curve shows an AUC (area under the curve) of 1.0 (Figure S16E). In summary, the proposed detection system is an effective molecular diagnostic toolkit, and its excellent discriminative capacity demonstrates its potential in clinical diagnosis.

CONCLUSIONS

Consequently, we developed a circular crRNA-mediated CRISPR molecular diagnostic (CRCD) toolkit. The integration of circular crRNA into this system effectively resolves the stability issues that are prevalent in traditional CRISPR-based systems. This novel detection platform shows a 10-fold increase in sensitivity upon exposure to RNase R compared to the conventional CRISPR system, highlighting its potential superiority as a component of the CRISPR toolkit. We then successfully integrated CRCD with a standard PCR technique, enabling the detection of synthesized HPV-16 plasmids at concentrations as low as 10 aM. In further clinical trials, our method demonstrated the ability to accurately detect clinical samples of HPV-16 and IVA. Furthermore, the potential of this system for practical point-of-care detection has been validated.

In this study, the current detection process still requires a certain amount of time, which may limit its application in some emergency situations. Therefore, optimizing the detection procedure, especially the rapid preparation of circular RNA, to reduce the detection time is an important direction for future research. Additionally, while the CRCD toolkit exhibits slightly superior specificity compared to the traditional CRISPR system, there remains a need to further enhance its specificity in order to broaden the application scenario. This enhancement may be achieved through more rigorous guide RNA selection and protein and crRNA engineering. In conclusion, this research proposes a new conformationally engineered crRNA for the construction of CRISPR molecular diagnostic platforms. Moreover, CRCD is a universal and robust nucleic acid detection method, which has potential clinical application in the detection of infectious diseases.

ASSOCIATED CONTENT

Supporting Information

The Supporting Information is available free of charge at https://pubs.acs.org/doi/10.1021/acs.analchem.4c06107.

Materials and reagents; PCR and RT-PCR amplification; statistical analysis; sequences of RNA used in this work; plasmid information of IVA gene; PAGE analysis of *cis*-cleavage; optimization of the CRCD sensing conditions; optimize the RT-PCR primer (PDF)

AUTHOR INFORMATION

Corresponding Authors

Min Qing − *Chongqing Research Center for Pharmaceutical Engineering, College of Pharmacy, Chongqing Medical University, Chongqing 400016, P. R. China;* orcid.org/0000-0001-9491-0360; Email: mindaqing@cqmu.edu.cn

Lijuan Bai − *Chongqing Research Center for Pharmaceutical Engineering, College of Pharmacy, Chongqing Medical University, Chongqing 400016, P. R. China; Department of Respiratory and Critical Care Medicine, the First Affiliated Hospital of Chongqing Medical University, Chongqing 400016, P. R. China;* orcid.org/0000-0001-9450-4581; Email: bailj1018@cqmu.edu.cn

Authors

Yueyuan Li − *Chongqing Research Center for Pharmaceutical Engineering, College of Pharmacy, Chongqing Medical University, Chongqing 400016, P. R. China*

Qianfang Hu − *Department of Respiratory and Critical Care Medicine, the First Affiliated Hospital of Chongqing Medical University, Chongqing 400016, P. R. China*

Meiqi Bai − *Chongqing Research Center for Pharmaceutical Engineering, College of Pharmacy, Chongqing Medical University, Chongqing 400016, P. R. China*

Complete contact information is available at: https://pubs.acs.org/10.1021/acs.analchem.4c06107

https://doi.org/10.1021/acs.analchem.4c06107
Anal. Chem. 2025, 97, 3617−3624

Author Contributions

All authors have given approval to the final version of the manuscript.

Notes

The authors declare no competing financial interest.

■ ACKNOWLEDGMENTS

This work was supported by National Natural Science Foundation of China (82072378, 81601856), Chongqing Talents: Exceptional Young Talents Project, China (CQYC202005015, cstc2021ycjhbgzxm0328), Natural Science Foundation of Chongqing, China (CSTB2024NSCQ-MSX0583), Discipline Talent Training Program of College of Pharmacy in Chongqing Medical University, China (YXY2021BSH04), and CQMU Program for Youth Innovation in Future Medicine, China (172020320220090 W0072).

■ REFERENCES

(1) Knott, G. J.; Doudna, J. A. *Sience* **2018**, *361* (6405), 866−869.
(2) Jinek, M.; Chylinski, K.; Fonfara, I.; Hauer, M.; Doudna, J. A.; Charpentier, E. *Science* **2012**, *337* (6096), 816−821.
(3) Garneau, J. E.; Dupuis, M. E.; Villion, M.; Romero, D. A.; Barrangou, R.; Boyaval, P.; Fremaux, C.; Horvath, P.; Magadán, A. H.; Moineau, S. *Nature* **2010**, *468* (7320), 67−71.
(4) Zhao, R.; Luo, W.; Wu, Y.; Zhang, L.; Liu, X.; Li, J. J.; Yang, Y. J.; Wang, L.; Wang, L. J.; Han, X. L.; Wang, Z. Z.; Zhang, J. H.; Lv, K.; Chen, T. M.; Xie, G. M. *Nucleic Acids Res.* **2023**, *51* (19), 10795−10807.
(5) Mohammad, N.; Katkam, S. S.; Wei, Q. S. *Angew. Chem., Int. Ed.* **2022**, *61* (50), No. e202213920.
(6) Hu, M. L.; Qiu, Z. Q.; Bi, Z. R.; Tian, T.; Jiang, Y. Z.; Zhou, X. M. *Proc. Natl. Acad. Sci. U.S.A.* **2022**, *119* (26), No. e2202034119.
(7) Samanta, D.; Ebrahimi, S. B.; Ramani, N.; Mirkin, C. A. *J. Am. Chem. Soc.* **2022**, *144* (36), 16310−16315.
(8) Moon, J.; Liu, C. C. *Nat. Commun.* **2023**, *14* (1), No. 7504.
(9) Tong, X. H.; Zhang, K.; Han, Y.; Li, T. L.; Duan, M.; Ji, R. J.; Wang, X. G.; Zhou, X.; Zhang, Y.; Yin, H. *Nat. Chem. Biol.* **2024**, *20* (7), 885−893.
(10) Chen, J. S.; Ma, E. B.; Harrington, L. B.; Da Costa, M.; Tian, X. R.; Palefsky, J. M.; Doudna, J. A. *Science* **2018**, *360* (6387), 436−439.
(11) Zetsche, B.; Gootenberg, J. S.; Abudayyeh, O. O.; Slaymaker, I. M.; Makarova, K. S.; Essletzbichler, P.; Volz, S. E.; Joung, J.; van der Oost, J.; Regev, A.; Koonin, E. V.; Zhang, F. *Cell* **2015**, *163* (3), 759−771.
(12) Stella, S.; Mesa, P.; Thomsen, J.; Paul, B.; Alcón, P.; Jensen, S. B.; Saligram, B.; Moses, M. E.; Hatzakis, N. S.; Montoya, G. *Cell* **2018**, *175* (7), 1856−1871.
(13) Nishimasu, H.; Yamano, T.; Gao, L. Y.; Zhang, F.; Ishitani, R.; Nureki, O. *Mol. Cell* **2017**, *67* (1), 139−147.
(14) Shi, J. Y.; Li, P. Y.; Huang, Y. M.; Wu, Y. Y.; Wu, J. W.; Huang, K. J.; Tan, X. C.; Ya, Y. *Chem. Eng. J.* **2024**, *483*, No. 149231.
(15) Gootenberg, J. S.; Abudayyeh, O. O.; Lee, J. W.; Essletzbichler, P.; Dy, A. J.; Joung, J.; Verdine, V.; Donghia, N.; Daringer, N. M.; Freije, C. A.; Myhrvold, C.; Bhattacharyya, R. P.; Livny, J.; Regev, A.; Koonin, E. V.; Hung, D. T.; Sabeti, P. C.; Collins, J. J.; Zhang, F. *Sience* **2017**, *356* (6336), 438−442.
(16) Li, S. Y.; Cheng, Q. X.; Wang, J. M.; Li, X. Y.; Zhang, Z. L.; Gao, S.; Cao, R. B.; Zhao, G. P.; Wang, J. *Cell Discovery* **2018**, *4*, No. 20.
(17) Nguyen, L. T.; Smith, B. M.; Jain, P. K. *Nat. Commun.* **2020**, *11* (1), No. 4906.
(18) Pandit, S.; Duchow, M.; Chao, W.; Capasso, A.; Samanta, D. *Angew. Chem.* **2024**, *136* (2), No. e202310964.
(19) Zuo, T. S.; Shen, C.; Xie, Z.; Xu, G. H.; Wei, F. D.; Yang, J.; Zhu, X. L.; Hu, Q.; Zhao, Z.; Tang, B. Z.; Cen, Y. *Nucleic Acids Res.* **2024**, *52* (19), 11884−11894.
(20) Ma, Y. Z.; Ya, Y. Y.; Wu, Y. Y.; Yan, J.; Huang, K. J.; Tan, X. C.; Duan, Y. *Int. J. Biol. Macromol.* **2024**, *282*, No. 137536.
(21) Ma, H. H.; Tu, L. C.; Naseri, A.; Huisman, M.; Zhang, S. J.; Grunwald, D.; Pederson, T. *J. Cell Biol.* **2016**, *214* (5), 529−537.
(22) Zhang, X.; Wang, X. L.; Lv, J.; Huang, H. X.; Wang, J. H.; Zhuo, M.; Tan, Z. H.; Huang, G. J.; Liu, J. W.; Liu, Y. C.; Li, M. R.; Lin, Q. X.; Li, L.; Ma, S. F.; Huang, T.; Lin, Y.; Zhao, X. Y.; Rong, Z. L. *Genome Biol.* **2023**, *24* (1), No. 145.
(23) Gao, Q.; Li, S. *Interdiscip. Med.* **2024**, *2* (1), No. e20230031.
(24) Rozners, E. *J. Am. Chem. Soc.* **2022**, *144* (28), 12584−12594.
(25) Yin, H.; Song, C. Q.; Suresh, S.; Wu, Q. Q.; Walsh, S.; Rhym, L. H.; Mintzer, E.; Bolukbasi, M. F.; Zhu, L. J.; Kauffman, K.; Mou, H. W.; Oberholzer, A.; Ding, J. M.; Kwan, S. Y.; Bogorad, R. L.; Zatsepin, T.; Koteliansky, V.; Wolfe, S. A.; Xue, W.; Langer, R.; Anderson, D. G. *Nat. Biotechnol.* **2017**, *35* (12), 1179−1187.
(26) Cromwell, C. R.; Sung, K.; Park, J.; Krysler, A. R.; Jovel, J.; Kim, S. K.; Hubbard, B. P. *Nat. Commun.* **2018**, *9*, No. 1448.
(27) O'Reilly, D.; Kartje, Z. J.; Ageely, E. A.; Malek-Adamian, E.; Habibian, M.; Schofield, A.; Barkau, C. L.; Rohilla, K. J.; DeRossett, L. B.; Weigle, A. T.; Damha, M. J.; Gagnon, K. T. *Nucleic Acids Res.* **2019**, *47* (2), 546−558.
(28) Rueda, F. O.; Bista, M.; Newton, M. D.; Goeppert, A. U.; Cuomo, M. E.; Gordon, E.; Kröner, F.; Read, J. A.; Wrigley, J. D.; Rueda, D.; Taylor, B. J. M. *Nat. Commun.* **2017**, *8*, No. 1610.
(29) Nelson, J. W.; Randolph, P. B.; Shen, S. P.; Everette, K. A.; Chen, P. J.; Anzalone, A. V.; An, M.; Newby, G. A.; Chen, J. C.; Hsu, A.; Liu, D. R. *Nat. Biotechnol.* **2022**, *40* (3), 402−410.
(30) Liu, L.; Li, W. B.; Li, J.; Zhao, D. D.; Li, S. W.; Jiang, G.; Wang, J.; Chen, X. X.; Bi, C. H.; Zhang, X. L. *ACS Synth. Biol.* **2023**, *12* (2), 350−359.
(31) Chen, L. L. *Nat. Rev. Mol. Cell Biol.* **2016**, *17* (4), 205−211.
(32) Zhang, L.; Liu, Q.; Guo, Y. C.; Tian, L. Y.; Chen, K. N.; Bai, D.; Yu, H. Y.; Han, X. L.; Luo, W.; Feng, T.; Deng, S. X.; Xie, G. M. *J. Nanobiotechnol.* **2024**, *22* (1), No. 189.
(33) Goodall, G. J.; Wickramasinghe, V. O. *Nat. Rev. Cancer* **2021**, *21* (1), 22−36.
(34) Zhou, R. Y.; Wu, Y. W.; Wang, W. X.; Su, W. J.; Liu, Y. C.; Wang, Y. M.; Fan, C. M.; Li, X. L.; Li, G. Y.; Li, Y.; Xiong, W.; Zeng, Z. Y. *Cancer Lett.* **2018**, *425*, 134−142.
(35) Jeck, W. R.; Sharpless, N. E. *Nat. Biotechnol.* **2014**, *32* (5), 453−461.
(36) Zhou, W. Y.; Cai, Z. R.; Liu, J.; Wang, D. S.; Ju, H. Q.; Xu, R. H. *Mol. Cancer* **2020**, *19* (1), No. 172.
(37) Fonfara, I.; Richter, H.; Bratovic, M.; Le Rhun, A.; Charpentier, E. *Nature* **2016**, *532* (7600), 517−521.
(38) Li, S. Y.; Cheng, Q. X.; Liu, J. K.; Nie, X. Q.; Zhao, G. P.; Wang, J. *Cell Res.* **2018**, *28* (4), 491−493.
(39) Anzalone, A. V.; Koblan, L. W.; Liu, D. R. *Nat. Biotechnol.* **2020**, *38* (7), 824−844.
(40) Roden, R.; Wu, T. C. *Nat. Rev. Cancer* **2006**, *6* (10), 753−763.
(41) Castellsagué, X. *Gynecol. Oncol.* **2008**, *110* (3), S4−S7.
(42) Pirog, E. C.; Lloveras, B.; Molijn, A.; Tous, S.; Guimerà, N.; Alejo, M.; Clavero, O.; Klaustermeier, J.; Jenkins, D.; Quint, W. G. V.; Bosch, F. X.; Alemany, L.; de Sanjosé, S.; Grp, R. H. T. S. *Mod. Pathol.* **2014**, *27* (12), 1559−1567.
(43) Bao, H.; Min, L.; Bu, F.; Wang, S.; Meng, J. *Interdiscip. Med.* **2023**, *1* (4), No. e20230021.
(44) Parrish, C. R.; Holmes, E. C.; Morens, D. M.; Park, E. C.; Burke, D. S.; Calisher, C. H.; Laughlin, C. A.; Saif, L. J.; Daszak, P. *Microbiol. Mol. Biol. Rev.* **2008**, *72* (3), 457−470.
(45) Wolff, G. G. *Vaccine* **2020**, *38* (2), 350−354.

https://doi.org/10.1021/acs.analchem.4c06107
Anal. Chem. 2025, 97, 3617−3624